Clinically Relevant Pathogens on Surfaces Display Differences in Survival and Transcriptomic Response in Relation to Probiotic and Traditional Cleaning Strategies

Jinglin Hu[1], Weitao Shuai[1], Jack T. Sumner[1], Anahid A. Moghadam[1], Erica M. Hartmann[*,1]

[1]Department of Civil and Environmental Engineering, Northwestern University, Evanston, IL 60208 USA

Abstract

Prolonged survival of clinically relevant pathogens on inanimate surfaces represents a major concern in healthcare facilities. Contaminated surfaces can serve as reservoirs of potential pathogens and greatly hinder the prevention of healthcare-associated infections. Probiotic cleaning using environmental microorganisms to promote inter-species competition has been proposed as an alternative to traditional chemical-based cleaning using antimicrobials. Probiotic cleaning seeks to take advantage of ecological principles such as competitive exclusion and utilize benign microorganisms to inhibit viable pathogens on indoor surfaces. However, limited mechanistic study has yielded direct evidence that enables the scientific community to understand the stress response, or microbe-microbe interactions between healthcare-associated pathogens and probiotic bacteria. Therefore, to bridge this knowledge gap, we combined transcriptomics and traditional microbiology techniques to investigate the differential impact of chemical-based and probiotic surface cleaners on the survival of *Acinetobacter baumannii* and *Klebsiella pneumoniae*, two clinically important pathogens. Although probiotic *Bacillus* included

in a commercialized All-Purpose Probiotic Cleaner persisted on surfaces for an extended period of time, surfaces contaminated with *A. baumannii* cleaned using chemical-based detergent with and without probiotic *Bacillus* showed no statistical difference in the viable colony forming units (CFUs) of *A. baumannii*. Similarly, for *Klebsiella pneumoniae*, there were negligible statistical differences in CFUs between probiotic and detergent cleaning scenarios. The transcriptome of *A. baumannii* with and without probiotic addition shared a high degree of similarity in overall gene expression, while the transcriptome of *K. pneumoniae* with and without probiotic addition differed in overall gene expression. Together, these results highlight the need to fully understand the underlying biological and ecological mechanisms for different pathogens and practical implications of probiotic indoor cleaning.

Keywords: probiotic cleaner; *Acinetobacter baumannii*; *Klebsiella pneumoniae*; transcriptomic response; indoor surface cleaning; infection prevention

1. *Introduction*

Acinetobacter baumannii and *Klebsiella pneumoniae* have been recognized as a major source of healthcare-associated infections associated with high morbidity and mortality rates due to their resistance to many antibiotics including carbapenems[1 2]. *Acinetobacter* and *Klebsiella* species are capable of contaminating and persisting on inanimate surfaces for up to several months [3], significantly increasing the risk of acquisition for hospitalized patients who are immunocompromised. Given the concern with transmission of infectious microorganisms including *Acinetobacter* and *Klebsiella*, many cleaning products contain added antimicrobials as disinfectants. However, questions remain about the extent to which chemicals, particularly antimicrobial products, reduce nosocomial infections and whether misuse of these products leads to antimicrobial resistance[4–6]. Several recent studies have demonstrated that cleaning using antimicrobials can effectively reduce microbial load on contaminated surfaces in health care facilities[7]. However, their effects on preventing disease transmission and reducing healthcare-acquired infections remain limited[8]. In addition to concerns about antimicrobial resistance, exposure to cleaning and disinfection agents can cause both acute and chronic health impacts. Healthcare workers with pre-existing respiratory illness, such as asthma, are particularly vulnerable[9]. As a result, an alternative strategy using microbiome manipulation draws increasing attention, seeking to promote inter-species competition between pathogens and probiotic microorganisms, namely *Bacillus*[10–14] , rather than using chemicals to combat pathogens in the built environment.

58 Falagas and Makris first proposed to use environmental probiotic microorganisms and/or
59 biosurfactants to suppress the colonization of nosocomial pathogens and subsequently reduce
60 nosocomial infections in healthcare facilities in 2009[13]. Since then, much work on the probiotic
61 cleaning potential of *Bacillus* has been performed[10–12,14]. *Bacillus* is a genus of bacteria
62 commonly found indoors[15]. Species of *Bacillus* are generally recognized as safe[16] , with a few
63 exceptions (e.g., *Bacillus anthracis*). In addition to its prevailing presence, *Bacillus* bacteria are
64 capable of forming spores[17] , which can remain viable for an extended period of time, making
65 them ideal for storing in detergents.
66
67 Probiotic cleaning seeks to take advantage of competitive exclusion and other ecological
68 principles to inhibit viable pathogens on surfaces[4,18], but there is limited direct evidence
69 documenting these phenomena, along with stress response, or microbe-microbe interactions
70 between probiotic and healthcare-associated pathogens. One major challenge is the technical
71 limitations of many techniques, e.g., transcriptomic sequencing of low biomass samples
72 collected from the built environment often suffers from a low signal-to-noise ratio. Therefore, to
73 obtain a fundamental mechanistic understanding of indoor cleaning strategies and their impacts
74 on microbial survival and interactions, we utilized microcosm chambers to simulate a simplified
75 built environment with greater than usual microbial load. We seek to quantify the effects of
76 probiotic cleaning on viability reduction of healthcare-associated pathogens (e.g., *A. baumannii*
77 and *K. pneumoniae*) and evaluate inter-species interactions between *Bacillus* contained in a
78 probiotic surface cleaner and healthcare-associated pathogens under ambient conditions and
79 elevated temperature and humidity. Cleaning and probiotic products represent a multi-billion-
80 dollar market and a critical tool in our arsenal against microbial infections. Being able to fully

81 understand microbe-chemical and microbe-microbe interactions will not only help determine the
82 most successful contexts for probiotic cleaning, but also lead to better future product
83 formulation.
84

85 ## 2. *Materials and Method*

86 ### *2.1. Microcosm set-up*

87 A commercially available All-Purpose Probiotic Cleaner (APPC) was obtained from Graz,
88 Austria. Clinical isolates of *Acinetobacter baumannii* (ABBL18) and *Klebsiella pneumoniae*
89 (CRE231) were provided by Dr. Alan Hauser, Northwestern University Feinberg School of
90 Medicine. To simulate a typical indoor surface environment, 24G stainless steel sheets were cut
91 into 2"x2" squares. *A. baumannii* (ABBL18) and *K. pneumonia*e (CRE231) isolates were grown
92 in 40 mL tryptic soy broth (TSB) for 23 hours at 30°C with continuous shaking to its mid log
93 phase. The APPC was filtered through a 0.22 μm syringe filter to create an All-Purpose Cleaner
94 (APC) without probiotic materials as a control. Vegetative *Bacillus spp*. (VB) culture was
95 prepared by mixing 0.1% APPC with TSB. This culture was incubated at 25°C for 23 hours with
96 continuous shaking. Cells (*Bacillus spp*., *A. baumannii and K. pneumoniae*) were harvested and
97 washed in phosphate-buffered saline (PBS) before inoculation.
98

99 A total of six testing scenarios for each pathogen (twelve groups in total) are specified as
100 follows:
101

102 Table 1 Testing scenarios for each pathogen (*A. baumannii* and *K. pneumoniae)* consisting of
103 four cleaning conditions, and two temperature and humidity conditions.

104

Cleaning Scenarios	Temperature and humidity conditions	
	25°C and 20% RH	37°C and 90% RH
Pathogen	Pathogen (A)	Pathogen (W)
Pathogen + APC	Pathogen + APC (A)	NA
Pathogen + APPC	Pathogen + APPC (A)	Pathogen + APPC (W)
Pathogen + VB	Pathogen + VB (A)	NA

105

106 Each 2"x2" stainless steel surface was first inoculated with 50 μL *A. baumannii* (corresponding
107 to 8.5×10^7 CFU) or 50 μL *K. pneumoniae* (corresponding to 1.0×10^8 CFU). 50 μL sterilized PBS
108 buffer, APC, APPC, or vegetative *Bacillus spp*. inoculum was added to create no-cleaning
109 control samples (ABBL18 or CRE231), chemical cleaning samples (ABBL18 + APC or CRE231
110 + APC), probiotic cleaning samples (ABBL18 + APPC or CRE231 + APPC), or vegetative
111 cleaning samples (ABBL18 + VB or CRE231 + VB), respectively. Following the introduction of
112 bacterial inoculum, all surfaces were transferred into autoclaved mason jars under two treatment
113 conditions: 1) ambient temperature (25°C) and relative humidity (20%), and 2) elevated
114 temperature (37°C) and relative humidity (>90%) with 10 mL of autoclaved milliQ water. All
115 microcosm chambers were stored in incubators maintained at 25°C or 37°C. Swab samples were
116 collected at three specific timepoints: 3 hours, 24 hours, and 72 hours following the inoculation
117 and cleaning. Triplicate samples were prepared for each combination of cleaning, timepoint, and
118 incubation conditions (Figure 1).

119

120 *2.2. Swab sample collection*

121 Swab samples were collected through a combination of dry and wet swabbing as performed
122 previously[19]. Each surface was first dry swabbed from left to right for seven times and the swab
123 was swirled into an aliquoted PBS buffer or RNAprotect Bacteria Reagent (Qiagen), for CFU
124 enumeration and RNA extraction, respectively. Surfaces were then wet swabbed for a total of 20
125 s, including 5 seconds of rinse and rewet. Finally, the swabs were left in 15 mL conical tubes and
126 vortexed for 10 seconds. 100 μL swab suspension along with its dilutions were spread onto
127 tryptic soy agar (TSA) and CHROM *Acinetobacter baumannii* selective agar and on MacConkey
128 agar as *Klebsiella pneumoniae* selective media[20] and incubated at 37°C. Numbers of colony
129 forming units (CFUs) were counted after three days.

130

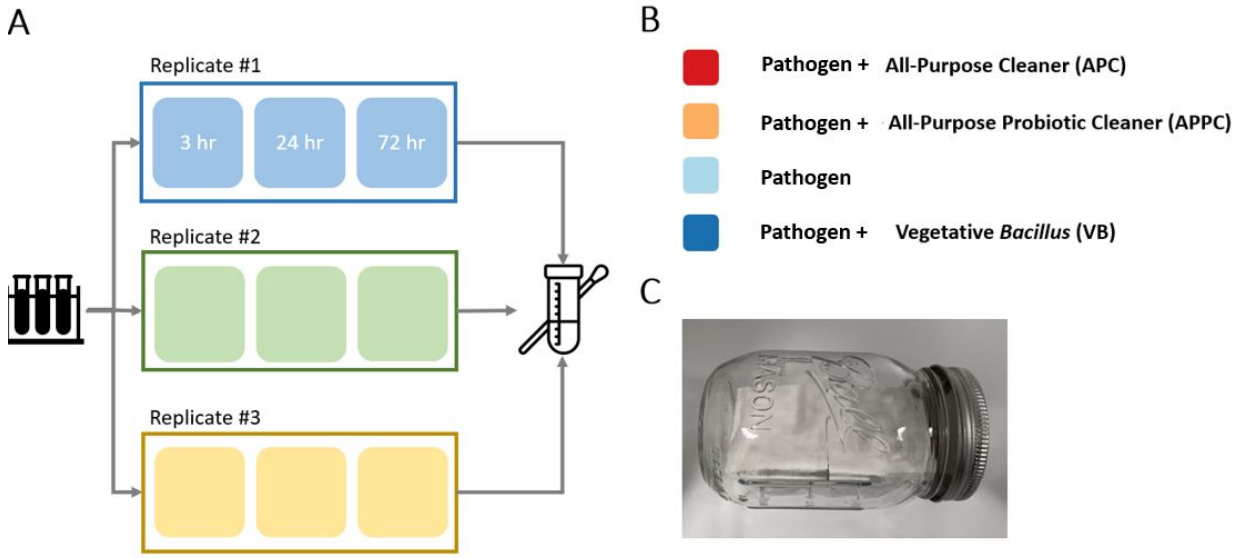

131

132 Figure 1. Microcosm experimental design (A) with four types of inoculums (B) containing
133 pathogen (*A. baumannii* or *K. pneumoniae*) and *Bacillus spp.* and sealed sterile
134 microcosm chamber maintained under ambient temperature and relative humidity (C).

135 The elevated temperature and humidity condition was maintained by adding 10 mL of
136 sterilized miliQ water into the sealed chamber.
137
138 2.3. *DNA extraction, sequencing, and construction of reference genomes*
139 To obtain draft genomes for RNA read mapping, 5 mL *A. baumannii* or *K. pneumoniae* and 15
140 mL *Bacillus spp*. DNA was extracted using the DNeasy PowerSoil Pro Kit (Qiagen) following
141 the manufacturer's instructions. DNA samples were submitted to the Microbial Genome
142 Sequencing Center (MiGS) for library construction and sequencing. KneadData v0.7.10
143 (https://bitbucket.org/biobakery/kneaddata/) was then used for raw sequence quality control and
144 contaminant removal with default parameters. Short reads were assembled into contigs using
145 SPAdes v3.14.1[21] and each reference genome was annotated using Prokka v1.14.6[22]. Additional
146 annotation of antibiotic and antimicrobial resistance genes were conducted using the
147 Comprehensive Antibiotic Resistance Database (CARD)[23]. Assembled contigs from All Purpose
148 Probiotic Cleaner were also binned into five metagenome-assembled genomes (MAGs) using
149 metaWRAP[24]. CheckM[25] was used to assess the quality of microbial genomes. Taxonomic
150 classification of each draft genome was determined by GTDB-Tk[26].
151
152 *2.4. RNA Extraction, Sequencing, and Data Processing*
153 Swab samples were stored in RNAprotect Bacteria Reagent under -80°C until extraction. RNA
154 was extracted using the RNeasy Mini Kit (Qiagen) following its recommended "Protocol 2:
155 Enzymatic lysis and mechanical disruption of bacteria", consisting of a 10 min treatment with 15
156 mg/mL lysozyme and 10 min beadbeating. Libraries were constructed at Northwestern NUSeq
157 using the Illumina Total RNA Prep with Ribo-Zero Plus, according to manufacturers' protocol. A

158 total of 56 samples (54 samples collected at various time points and cleaning scenarios, one kit
159 control, and one sample prepared for future between-batch normalization). Samples were
160 sequenced using a HiSeq4000 with 50 bp single end reads.

161 Reference genomes constructed from whole genome sequencing were used for RNA mapping.
162 Raw sequence files were processed using trim_galore v0.6.6
163 (https://www.bioinformatics.babraham.ac.uk/projects/trim_galore/) and Kneaddata v0.7.10
164 (https://bitbucket.org/biobakery/kneaddata/) to remove sequence adapters, low quality reads, and
165 contaminants. Sortmerna v4.2.0[27] was used to filter rRNA reads against the silva-bac-16s-id90
166 and silva-bac-23s-id98 databases. HISAT2 v2.1.0[28] was used to build local indices and map
167 short reads onto reference draft genomes. Transcript abundances were quantified using
168 featureCounts v2.0.1[29]. Differentially expressed genes (DEGs) were identified by DESeq2[30] at a
169 significance level of 0.05 (Benjamini-Hochberg adjusted p-value). BlastKOALA (KEGG
170 Orthology And Links Annotation) was used for K number assignment followed by Prokka
171 annotation[31]. KEGG pathway enrichment analysis was further conducted using ClusterProfiler[32].
172 Statistical analysis, including Welch's paired two sample *t*-test, principal component analysis
173 (PCA), and permutational multivariate analysis of variance (PERMANOVA, 9,999
174 permutations) were conducted in R (version 4.1.2, 2021-11-01).
175

176 ## 3. ***Results and Discussion***

177 ### ***3.1.*** *Survival of* A. baumannii *and* K. pneumoniae *under four cleaning scenarios and two*
178 *temperature/humidity conditions*

179 We quantified the colony forming units (CFUs) of *Acinetobacter baumannii* and *Klebsiella*
180 *pneumoniae* (using CHROM selective agar for *Acinetobacter baumannii* and MacConkey agar

181 for *Klebsiella pneumoniae*) to examine their survival under ambient and wet conditions in
182 combination with four cleaning strategies: 1) no cleaning (ABBL18 or CRE231), 2) chemical
183 surface cleaning with All-Purpose Cleaning (ABBL18 + APC or CRE231 + APC), 3) probiotic
184 surface cleaning with All-Purpose Probiotic Cleaner (ABBL18 + APPC or CRE231 + APPC), 4)
185 and probiotic surface cleaning with vegetative *Bacillus spp*. (ABBL18 + VB or CRE231 + VB).
186 Under the circumstances where *Bacillus* were introduced through APPC and VB cleaning, total
187 CFUs were quantified using TSA.
188
189 Over the course of 3 days, we observed a maximum $\log_{10}$ reduction of 8.75 for *A. baumannii*
190 (ABBL18 + APC and ABBL18 + APPC under ambient condition) and 7.42 for *K. pneumoniae*
191 (CRE231, CRE231 + APC and CRE231 +APPC). A minimum $\log_{10}$ reduction of 3.75 for *A.*
192 *baumannii* (ABBL18 under elevated temperature and humidity) and 2.26 for *K. pneumoniae*
193 (CRE231 under elevated temperature and humidity). Under ambient conditions, both APC and
194 APPC demonstrated a near-complete inactivation of *A. baumannii* within 72 hours (<LOD) and
195 complete inactivation for *K. pneumoniae*. Although the survival of *A. baumannii* between APPC
196 and APC are not statistically significant ($p>0.05$, Figure S1), APPC cleaning at 24 hours showed
197 1.43 greater $\log_{10}$ reduction compared to APC (Figure 2A). The reduction of *A. baumannii* was
198 largely attributed to the chemical component; however, APPC might be able to achieve a near-
199 complete removal of *A. baumannii* within a shorter time frame compared to the use of chemical-
200 based APC alone. Differences in the survival of *K. pneumoniae* between APPC, APC and no-
201 cleaning scenarios was not statistically significant ($p>0.05$, Figure S1), with only 0.77 greater
202 $\log_{10}$ reduction in APPC compared to APC at 24 hours. The fact that *K. pneumoniae* was unable
203 to persist on the surface without any cleaning product under ambient conditions indicated that

204 chemical components in the cleaning product only had marginal contribution to *K. pneumoniae*
205 inactivation.
206
207 Surfaces cleaned with APPC were also gradually dominated by *Bacillus spp*. due to the
208 decreasing absolute abundance of the pathogen population. This persistence of *Bacillus spp*. on
209 surfaces was observed under both ambient and elevated humidity and temperature (Figure 2). In
210 contrast to the spores included in APPC, *Bacillus spp*. introduced as vegetative cells (ABBL18 +
211 VB) were gradually taken over by the *A. baumannii* population. In contrast, for CRE231 + VB
212 the cleaned surface was still dominated by *Bacillus spp* over *K. pneumoniae* (Figure 2A).
213 Without the use of chemical-based surface cleaner (ABBL18 and ABBL18 + VB), *A. baumannii*
214 showed comparable CFUs at all time points ($p > 0.05$). Samples with and without APPC
215 cleaning under elevated temperature and humidity showed significantly greater viable
216 populations of *A. baumannii* ($p<0.01$, Figure S1A), compared to ambient pairs. The same trend
217 was observed for *K. pneumoniae* (Figure 2B), although paired *t*-tests showed low or no
218 significance (Figure S1B). This result suggests greater potential health risks and infectious
219 disease burdens in developing regions with a humid and hot climate and limited climate
220 control[33].

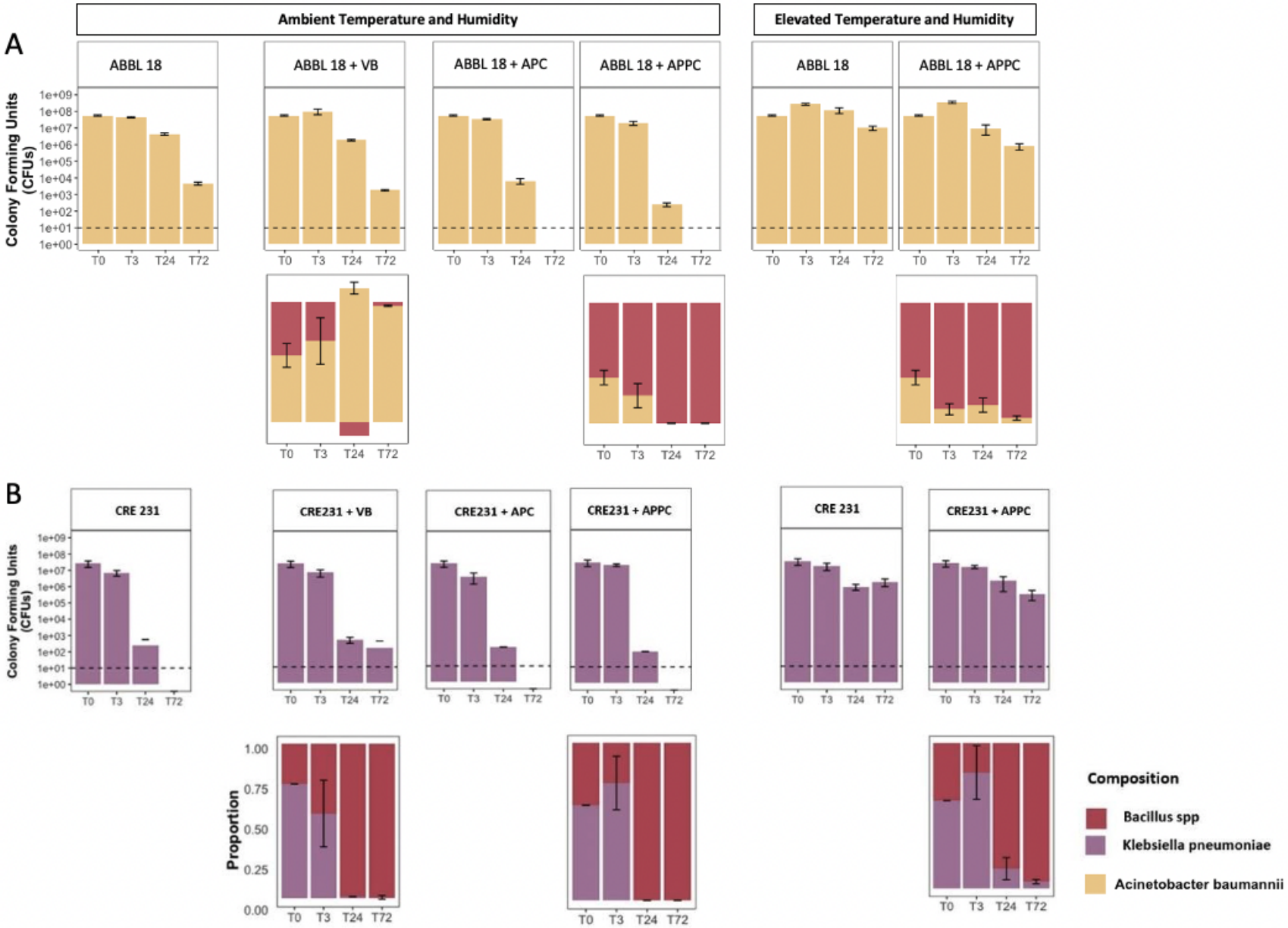
A
Ambient Temperature and Humidity
Elevated Temperature and Humidity
ABBL 18
ABBL 18 + VB
ABBL 18 + APC
ABBL 18 + APPC
ABBL 18
ABBL 18 + APPC
Colony Forming Units (CFUs)
1e+09
1e+08
1e+07
1e+06
1e+05
1e+04
1e+03
1e+02
1e+01
1e+00
T0
T3
T24
T72
B
CRE 231
CRE231 + VB
CRE231 + APC
CRE231 + APPC
CRE 231
CRE231 + APPC
Proportion
1.00
0.75
0.50
0.25
0.00
Composition
Bacillus spp
Klebsiella pneumoniae
Acinetobacter baumannii

221

222 Figure 2. Colony forming units (CFU) of pathogens and composition of surface microbial community under four cleaning
223 scenarios and two temperature and humidity conditions. CFUs of pathogens were counted on day 3 of incubation (37°C)
224 on their selective media while total CFUs (pathogen and *Bacillus spp.*) were obtained from TSA. The proportions of *A.*
225 *baumannii* and *K. pneumoiae* were calculated as the ratio between CFU from their selective media and CFU from TSA.
226 The proportion of *Bacillus spp.* was calculated as $\mathbf{1} - \frac{\boldsymbol{CFU(CHROM)}}{\boldsymbol{CFU(TSA)}}$. Dashed lines represent a limit of detection (LOD) of 10
227 CFU.

228 * Due to possible technical variation, the proportion of *A. baumannii* exceeded 1 at T24 for ABBL18 + VB.

229 *3.2. Overview of whole genome sequencing and metatranscriptomic data*

230 Sequencing of the *A. baumannii* (ABBL18) isolate generated 3.72 million reads with an average
231 read length of 136 bp. Reads were assembled into contigs with a N50 of 141,238 bp. Sequencing
232 of *K. pneumoniae* (CRE231) generated 4.4 million reads with an average rate of 145 bp. Reads
233 were assembled into contigs with a N50 of 113,698 bp. Sequencing of the All-Purpose Probiotic
234 Cleaner resulted in 16.49 million reads with an average read length of 139 bp, after quality
235 trimming and contaminant removal. Reads were assembled into contigs with a N50 of 143,313
236 bp. Open reading frame (ORF) identification recognized 4,039, 5,823, and 22,429 coding regions
237 for *A. baumannii, K. pneumoniae,* and APPC, respectively, 2,253, 4052, and 13,339 of which
238 were functionally annotated (not as "hypothetical protein") via Prokka. Among these annotated
239 regions for *A. baumannii, K. pneumoniae,* and APPC assemblies, 2,150, 3,675, and 11,594 were
240 classified into one or more KEGG Orthologs respectively. Contigs from APPC reads were
241 binned into five groups with completeness > 90%, and contamination < 5%. All five bins were
242 classified as *Bacillus* species as shown in Table 2.

243

244 Table 2. *Bacillus* genome binning and taxonomic assignment.

Bin	**Completeness (%)**	**Contamination (%)**	**GC (%)**	**Size (Mbp)**	**Taxonomic Classification**
1	90.58	1.883	0.351	4.74	*Bacillus cereus*
2	96.43	1.489	0.466	3.60	*Bacillus velezensis*
3	99.11	0.148	0.436	4.11	*Bacillus subtilis*

4	98.21	0.087	0.461	4.28	*Bacillus licheniformis*
5	99.08	0.207	0.416	3.57	*Bacillus safensis*

245

246 RNA samples containing *A. baumannii* or *K. pneumoniae* were collected for up to 72 hours of
247 surface inoculation. Biological triplicates were collected for each condition and an average of
248 12.73 ± 3.83 and 11.03 ± 4.98 million reads with an average read length of 49 bp were recovered
249 for *A. baumannii* and *K. pneumoniae* experiments, respectively, after removing low-quality
250 reads, contaminated sequences, adapters, and rRNA. The average mapping rate using HISAT2
251 was 98.20% ± 1.06% for experiments with *A. baumannii* and 96.40% ± 10.24% for experiments
252 with *K. pneumoniae* (Figure S2). Percentages of reads mapped onto *A. baumannii* and *Bacillus*
253 genomes vary across four cleaning scenarios; VB samples containing vegetative *Bacillus spp*. on
254 average had 40.53% ± 6.07% reads mapped onto *Bacillus* reference genomes, whereas this
255 number for APPC samples was only 0.56% ± 0.75%. A similar trend was observed in
256 experiments with *K. pneumoniae* and *Bacillus spp*. CRE231 + VB samples containing vegetative
257 *Bacillus spp*. on average had 40.52% ±16.83% reads mapped onto *Bacillus* reference genomes;
258 however, this number was only 1.00 ±1.08% for APPC samples. Thus, these data suggest that the
259 majority of *Bacillus* in the probiotic product were likely to remain as spores throughout the
260 inoculation. Due to this insufficient coverage of *Bacillus* transcriptome in APPC samples, our
261 transcriptomic analysis is composed of quantitative comparisons for the *A. baumannii* and *K.*
262 *pneumoniae* transcriptomes and qualitative evaluations for *Bacillus spp*.

263

264 3.3. *Transcriptomes of* A. baumannii *and* K. pneumoniae *clustered into distinct groups*
265 *determined by cleaning and physical conditions*
266
267 Prior to conducting principal component analysis (PCA), read count data were transformed to
268 remove the dependence of the variance on the mean. PCA of the transformed (variance
269 stabilization) read counts belonging to *A. baumannii* indicated that the expression of *A.*
270 *baumannii* clustered into three distinct groups based on cleaning scenarios and physical
271 conditions (Figure 3A). Clustering of read counts from *K. pneumoniae* is more distinct for
272 different time points and physical conditions (Figure S2) compared to cleaning scenarios and
273 physical conditions (Figure 3C). PERMANOVA (9,999 permutations) revealed that temperature
274 and humidity ($p<0.001$), cleaning ($p<0.001$), and time ($p<0.001$) explained 12%, 30%, and 9%
275 of the variance for A. *baumannii* read counts, and 29%, 10%, and 12% for *K. pneumoniae* read
276 counts, respectively. Gene expression profiles of *A. baumannii* with detergent cleaning (APPC
277 and APC) are more similar to each other than they were to those without detergent (ABBL18 and
278 VB). Temperature and humidity conditions also affected the expression of *A. baumannii* under
279 the no-cleaning condition, but this impact was minimal when APPC was used. On the contrary,
280 the temperature and humidity strongly affected the gene expression profiles of *K. pneumoniae*
281 strongly, and the impact was more pronounced as the cleaning time extended from 3 hours to 24
282 and 72 hours.
283
284 Using no-cleaning samples (ABBL18 or CRE231) as the reference transcriptome, genes with
285 absolute $\log_2$ fold change values greater than or equal to 1 as calculated by DESeq2 were
286 considered as differentially expressed (Benjamini-Hochberg adjusted p-value ≤ 0.05). 414, 522,

287 and 634 genes of *A. baumannii* and 578, 145, and 57 genes of *K. pneumoniae* were found to be
288 differentially expressed in APC, APPC, and VB samples, respectively. The transcriptome of *A.*
289 *baumannii* with APC and APPC shared the highest level of similarity and consequently, the
290 smallest number of differentially expressed genes (APPC vs APC, Figure 3B). In the case of *K.*
291 *pneumoniae*, VB samples were the most similar to no-cleaning samples. Consistent with
292 previous PCA analysis, expression of *A. baumannii* under ambient and elevated temperature and
293 humidity conditions are drastically different from each other (1298 DEGs, Figure 3B) whereas
294 this difference in transcriptome diminished when APPC was used (133 DEGs). The high impact
295 of elevated temperature and humidity persisted for *K. pneumoniae* even when APPC was applied
296 (1828 and 1838 DEGs with or without APPC, Figure 3D). Since the transcriptome of *K.*
297 *pneumoniae* under APPC cleaning was fairly similar to the no-cleaning scenario, their similar
298 response to elevated temperature and humidity could be expected. Samples collected at various
299 time points throughout the microcosm inoculation also showed that much of the temporal
300 variation in gene expression occurred within 24 hours of surface cleaning and the number of
301 differentially expressed genes of the 72-hour samples decreased from 211 to 21 for A. *baumannii*
302 and from 876 to 19 for *K. pneumoniae* when compared to 3-hour and 24-hour samples. Similar
303 trends of differentially expressed gene numbers over time were observed in the read counts from
304 vegetative *Bacillus* (Figure S4), where no gene was considered to be differentially expressed
305 within 24 hours based on the criteria described above.

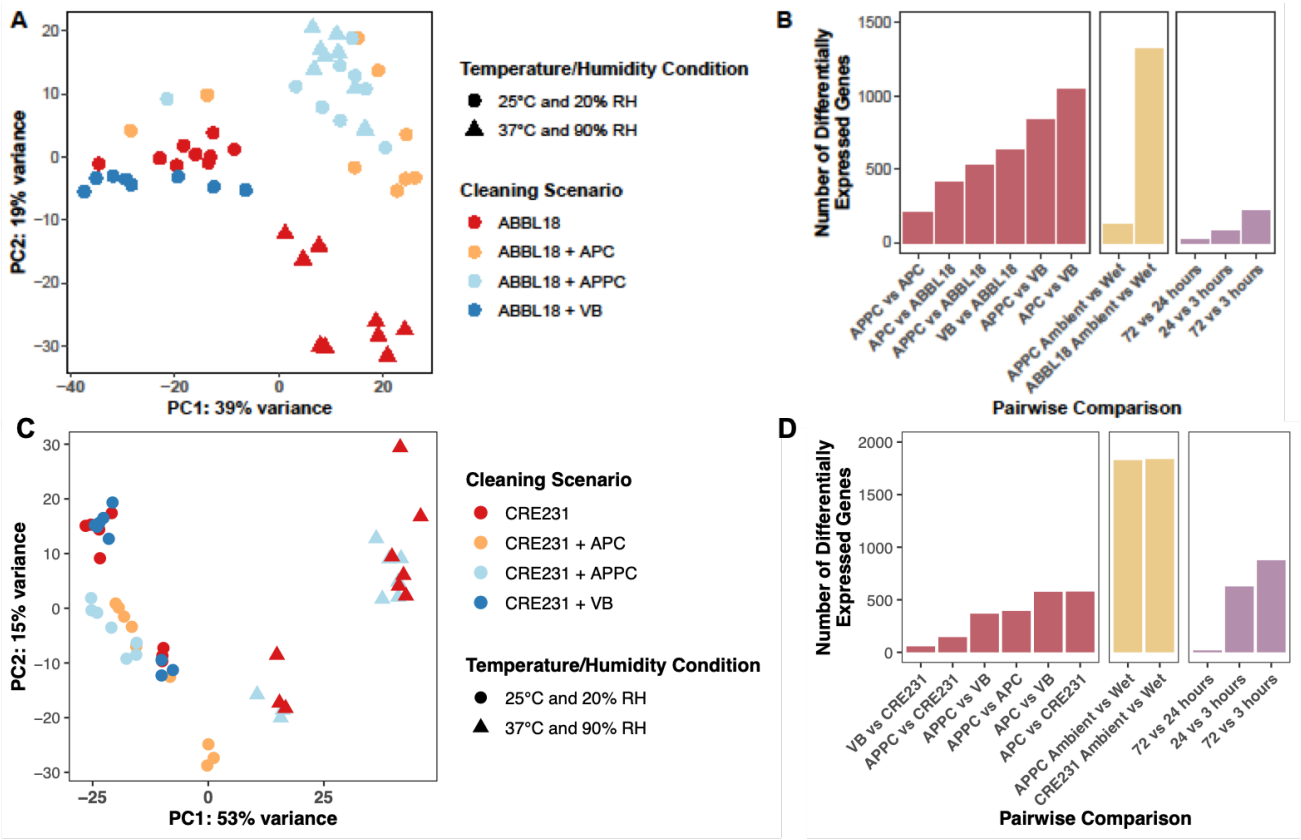

Figure 3. Principal component analysis on variance stabilized *Acinetobacter baumannii* (A) and *Klebsiella pneumoniae* (C) read counts and number of differentially expressed genes of 11 pairwise comparisons for *Acinetobacter baumannii* (B) and *Klebsiella pneumoniae* (D) experiments. Samples were color-coded based on cleaning conditions; each point (dot or triangle) represents its corresponding temperature and humidity condition.

311 *3.4. KEGG pathway enrichment profiles revealed different metabolic response under different*
312 *cleaning scenarios*
313
314 26 KEGG pathways related to metabolism (pyruvate, pyrimidine, purine, propionate, histidine,
315 fatty acids, etc.), translation (ribosome and aminoacyl-tRNA biosynthesis), energy production
316 (oxidative phosphorylation), and membrane transport (ABC transporters, and bacterial secretion
317 system) were positively enriched with a statistical significance in samples containing vegetative
318 *Bacillus* (ABBL18 + VB), compared to *A. baumannii* alone (ABBL18). Ribosome was the most
319 significant pathway, with 42 up-regulated genes. When vegetative *Bacillus spp*. were present,
320 protein synthesis of *A. baumannii* was likely promoted to achieve a large demand for surface
321 competitions. On the other hand, three pathways (geraniol degradation, fatty acid metabolism,
322 and valine, leucine, and isoleucine degradation) were positively enriched in samples with
323 chemical-based detergent cleaning (ABBL18 + APC and ABBL18 + APPC), indicating that the
324 *A. baumannii* population overall repressed metabolic activities and adaptively reduced synthesis
325 in response to environment constraints associated with detergent cleaning (Figure 4A).
326
327 11 KEGG pathways related to metabolism (citrate cycle, pyruvate, tyrosine, histidine, starch,
328 etc.), antibiotic resistance (cationic antimicrobial peptide resistance), and biofilm formation were
329 positively enriched with a statistical significance in samples containing vegetative *Bacillus*
330 (CRE231 + VB), compared to *K. pneumoniae* alone (CRE231). The TCA cycle was the most
331 significant pathway with 26 up-regulated genes (p-adjusted < 0.001, NES 2.36). Genes involved
332 in two-component systems and membrane transport (ABC) were upregulated in samples treated
333 with probiotic or detergent cleaners but not in samples containing vegetative *Bacillus* (CRE231).

This suggests that chemical detergents, rather than *Bacillus*, induce environmental sensing and response mechanisms in *K. pneumoniae*.

Differential expression of metabolic genes by *K. pneumoniae* was observed in each treatment group relative to no-cleaning controls. Carbon metabolism genes were up-regulated in each treatment group; however, the exact carbon processing pathways differed between groups. TCA cycle, pyruvate, starch and sucrose metabolism genes were up-regulated in samples containing vegetative *Bacillus* (CRE231 + VB) or detergent cleaner (CRE231 + APC) but not in samples treated with probiotic cleaner (CRE231 + APPC), suggesting a non-specific stress response. In contrast, no pathways were mutually and specifically enriched in samples containing vegetative *Bacillus* (CRE231 + VB) or probiotic cleaner (CRE231 + APPC), which is likely influenced by the diminished transcriptional landscape of *Bacillus* in probiotic cleaner (Figure S2). This suggests that vegetative *Bacillus* and cleaning products induce alternative though overlapping carbon metabolism networks in *K. pneumoniae*. Indeed, increased expression of biosynthetic pathways (glyoxylate cycle, carbon fixation) suggests vegetative *Bacillus* may promote anabolic competency in *K. pneumonia*. More research is needed to determine the role of metabolic manipulation with probiotics.

3.5. Different cleaning scenarios induced differential expression of genes associated with stress response and competition

Iron acquisition through siderophores is believed to be one of the key mechanisms of inter-species competitive exclusion[34]. Several genes responsible for siderophore synthesis, export, and

357 reception (e.g., aerobactin, anguibactin, and enterobactin) were slightly up-regulated in samples
358 with detergent cleaning (Figure S5A) but down-regulated in samples containing vegetative
359 *Bacillus spp*. in *A. baumannii* experiments. Although bacteria with multiple siderophore
360 receptors can gain competitive advantages in social competition through siderophore cheating[35],
361 the down-regulation of siderophore-related genes in these samples was likely due to utilization of
362 iron originating from lysed cell debris, especially from *Bacillus spp*., rather than active
363 competition through siderophore cheating, given the inability of vegetative *Bacillus spp*. to
364 persist on surfaces (Figure 2A). For *K. pneumoniae* experiments, no siderophore-related gene
365 was differentially expressed under the three cleaning scenarios (Figure S6A, *iutA*, *fepA*, and *fepC*
366 $\log_2$ fold change absolute values < 1). The fact that *Bacillus* took over the surface in the presence
367 of *K. pneumoniae* is likely related to *K. pneumoniae*'s inability to persist on the surface even
368 without any cleaning (Figure 2B). Additionally, transformed *Bacillus spp*. read counts unveiled
369 the predominant involvement of petrobactin as the primary siderophore in *Bacillus spp*. iron
370 acquisition. Genes related to the synthesis, and export of *Acinetobacter*- and *Klebsiella*-
371 associated siderophores (e.g., aerobactin, anguibactin, and enterobactin) were only occasionally
372 expressed (Figure S7), further reducing the likelihood of having siderophore cheating on
373 surfaces.
374
375 In addition to iron acquisition, genes related to Type VI Secretion Systems (T6SS), Type IV or
376 Type 1 Pili, and biofilm formation were shown to have important implications in inter-species
377 competition, virulence expression, and starvation response in *A. baumannii* or *K. pneumoniae*
378 [34,36,37]. Genes associated with T6SS and Type IV Pili were slightly upregulated in APPC, APC,
379 and VB samples for *A. baumannii* with varying statistical significance (Figure S5). Compared to

380 APC and APPC, a series of genes related to poly-beta-1,6-N-acetyl-D-glucosamine (PGA)
381 production, a biofilm adhesin polysaccharide[38,39], were up-regulated in the presence of vegetative
382 *Bacillus spp*. The increased expression of the *pgaABCD* operon with roles in surface binding and
383 maintaining biofilm structure stability[38,39] suggested greater potential for PGA production and
384 subsequent biofilm activities in samples containing both *A. baumannii* and *Bacillus spp*. In
385 contrast, genes related to T6SS and Type 1 Pili had negligible differences under different
386 cleaning scenarios for *K. pneumoniae* (Figure S6B,D). Additionally, only a few biofilm
387 formation related genes were differentially expressed under different cleaning scenarios
388 compared to non-cleaning samples for *K. pneumoniae*. Using absolute $\log_2$ fold change value ≥ 1
389 as threshold, eight genes were differentially expressed (four up-regulated, four down-regulated)
390 in chemical cleaner (APC) samples, two genes were differentially expressed (one up-regulated,
391 one down-regulated) in probiotic cleaning (APPC) samples, and five genes were differentially
392 expressed (one up-regulated and four down-regulated) in vegetative *Bacillus* (VB) samples
393 (Figure S7C). Lack of shared differentially expressed genes across cleaning scenarios with either
394 chemical substances nor *Bacillus* indicated nonspecific response of *K. pneumoniae* biofilm
395 formation towards different stressors. As biofilm formation is a complex process with an
396 important role in pathogenesis, more detailed studies in light of biofilm formation prevention for
397 various pathogenic species through different cleaning strategies are needed.
398
399 Meanwhile, several genes encoding efflux pumps were differentially expressed in APC and
400 APPC samples with *A. baumannii*, including up-regulated *mexJ* and *mexK*, which encode the
401 membrane fusion protein and the inner membrane resistance-nodulation-division (RND)
402 transporter of the MexJK multidrug efflux protein[40] , as well as down-regulated transcriptional

403 repressors of RND-type efflux pumps (e.g., *nalD*[41], and *adeN*[42]). In samples containing *A.*
404 *baumannii* and vegetative *Bacillus spp*., we observed an increased expression of *abaF*, a gene
405 encoding fosfomycin resistance. The effects of probiotic cleaner on *K. pneumoniae* antibiotic
406 resistance gene expression were much less pronounced, as only the *kpnF* gene ($\log_2$ fold change
407 = -1.09) belonging to major facilitator superfamily (MFS) antibiotic efflux pump and *uhpT* gene
408 with mutation conferring resistance to fosfomycin were slightly down-regulated ($\log_2$ fold
409 change = -1.01) in APPC samples (Figure 4E). However, no genetic determinants of fosfomycin
410 biosynthesis were identified from *Bacillus spp*. reference genomes. Although bacterial
411 multidrug resistance (MDR) efflux pumps are intensively studied for their profound impacts in
412 reducing antibiotic and antimicrobial susceptibilities, efflux pumps also alter transcriptomic
413 response related to central metabolism, pathogenicity, environmental sensing, and stress
414 response[43]. For example, the disruption of *abaF* in *A. baumannii* not only resulted in an increase
415 in fosfomycin susceptibility but also a decrease in biofilm formation and virulence[44]. *arnT* and
416 *pmrF* genes associated with peptide antibiotic resistance were up-regulated in APC samples for
417 *K. pneumoniae*, which could be induced by the chemical cleaning product.
418
419 Lastly, both APC and APPC showed pronounced downregulation of genes related to sulfur
420 metabolism, particularly those induced by sulfur starvation, but the expression of these genes
421 remained constant when no detergent was used for *A. baumannii* (Figure 4C). These genes
422 include a NADPH-dependent FMN reductase (*ssuE*) that was down-regulated by 35.13 fold in
423 APPC and 34.62 fold in APC, and upregulated by 1.30 fold in VB (adjusted p-value > 0.05), as
424 well as a *tauABCD* operon known to facilitate the utilization of taurine as an alternative sulfur
425 source under sulfate-deprived environment[45]. Similar down-regulation of sulfonate assimilation

426 genes (*ssuA*, *ssuB*, *ssuC*, *ssuD*, etc.) was observed under elevated temperature and humidity
427 conditions with APPC (Figure 5C). Owing to the presence of anionic surfactants in liquid
428 detergent products, such as sodium lauryl ether sulfate (SLES)[46], these sulfate starvation genes
429 were likely suppressed in APC and APPC samples. This observation is consistent with studies
430 that illustrated the overexpression of *tauABCD* and *ssuEADCB* genes induced by sulfate
431 shortage[47]. Additionally, bacterial utilization of SLES facilitated by *Citrobacter braakii* [48] and a
432 consortium of *Acinetobacter calcoacetiacus*, *Klebsiella oxytoca*, and *Serratia odorifera*[46] has
433 also been reported in previous studies and may contribute to the persistence of microbial
434 communities associated with hospital sinks[49]. The molybdenum cofactor biosynthesis operon
435 genes *moaABCDE*[50] were slightly down-regulated in APC and VB samples but not in APPC
436 samples for *K. pneumoniae* (Figure 4F). Most sulfur metabolism and antimicrobial resistance
437 related genes were not differentially expressed in APPC samples for *K. pneumoniae* but were
438 differentially expressed at different levels of significance in APC or VB samples. It is possible
439 that the dormant *Bacillus* cells in APPC were buffering the stress caused by chemical cleaner
440 while the vegetative *Bacillus* cells introduced competition pressure on the surfaces, as mentioned
441 previously. Further studies on the inter-species interaction between dormant or vegetative
442 *Bacillus* with different pathogens are needed to facilitate the development of probiotic cleaning
443 strategies.

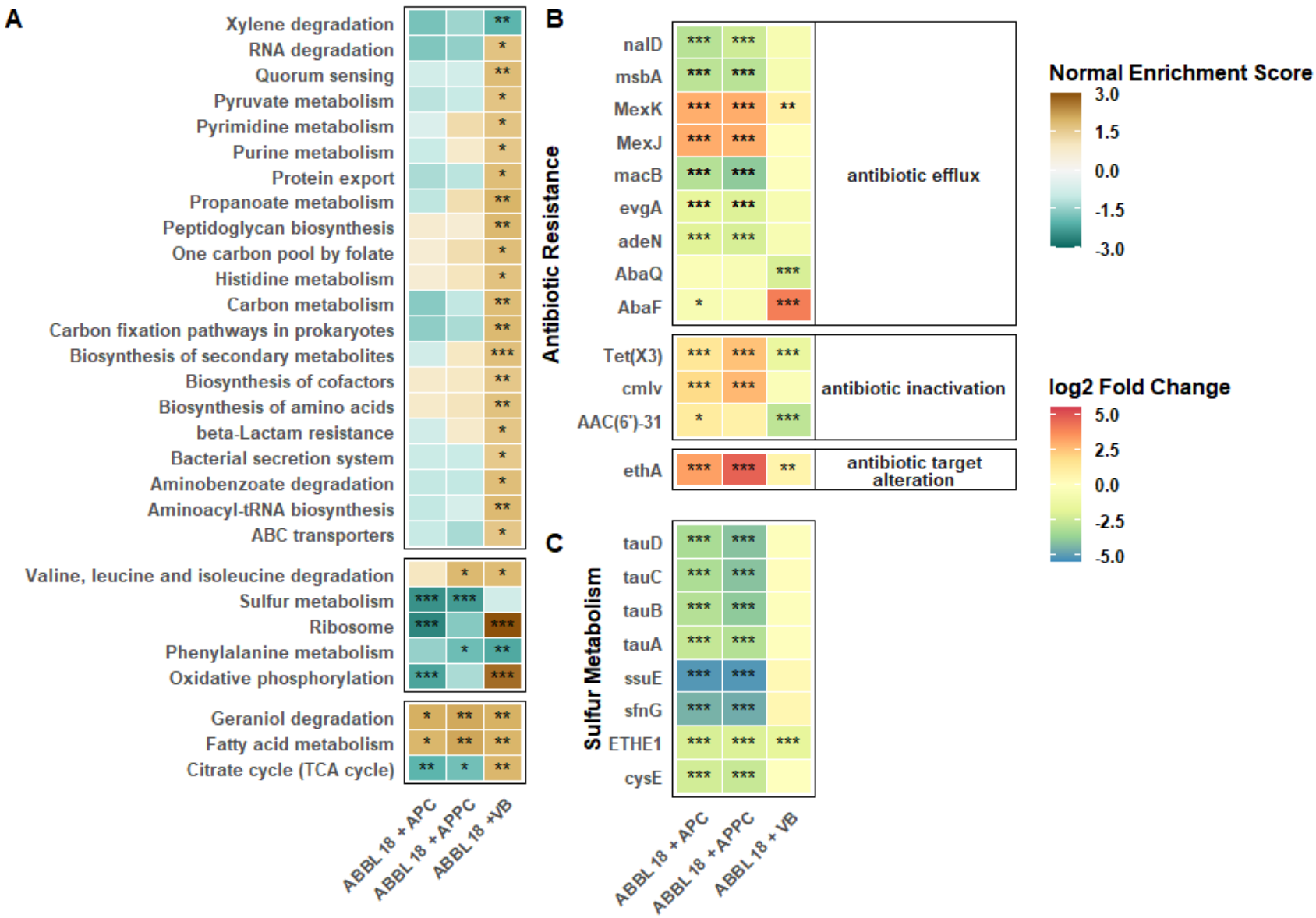
A
Xylene degradation
RNA degradation
Quorum sensing
Pyruvate metabolism
Pyrimidine metabolism
Purine metabolism
Protein export
Propanoate metabolism
Peptidoglycan biosynthesis
One carbon pool by folate
Histidine metabolism
Carbon metabolism
Carbon fixation pathways in prokaryotes
Biosynthesis of secondary metabolites
Biosynthesis of cofactors
Biosynthesis of amino acids
beta-Lactam resistance
Bacterial secretion system
Aminobenzoate degradation
Aminoacyl-tRNA biosynthesis
ABC transporters
Valine, leucine and isoleucine degradation
Sulfur metabolism
Ribosome
Phenylalanine metabolism
Oxidative phosphorylation
Geraniol degradation
Fatty acid metabolism
Citrate cycle (TCA cycle)
ABBL 18 + APC
ABBL 18 + APPC
ABBL 18 +VB
B
Antibiotic Resistance
naID
msbA
MexK
MexJ
macB
evgA
adeN
AbaQ
AbaF
antibiotic efflux
Tet(X3)
cmlv
AAC(6')-31
antibiotic inactivation
ethA
antibiotic target alteration
C
Sulfur Metabolism
tauD
tauC
tauB
tauA
ssuE
sfnG
ETHE1
cysE
ABBL 18 + APC
ABBL 18 + APPC
ABBL 18 + VB
Normal Enrichment Score
3.0
1.5
0.0
-1.5
-3.0
log2 Fold Change
5.0
2.5
0.0
-2.5
-5.0

444

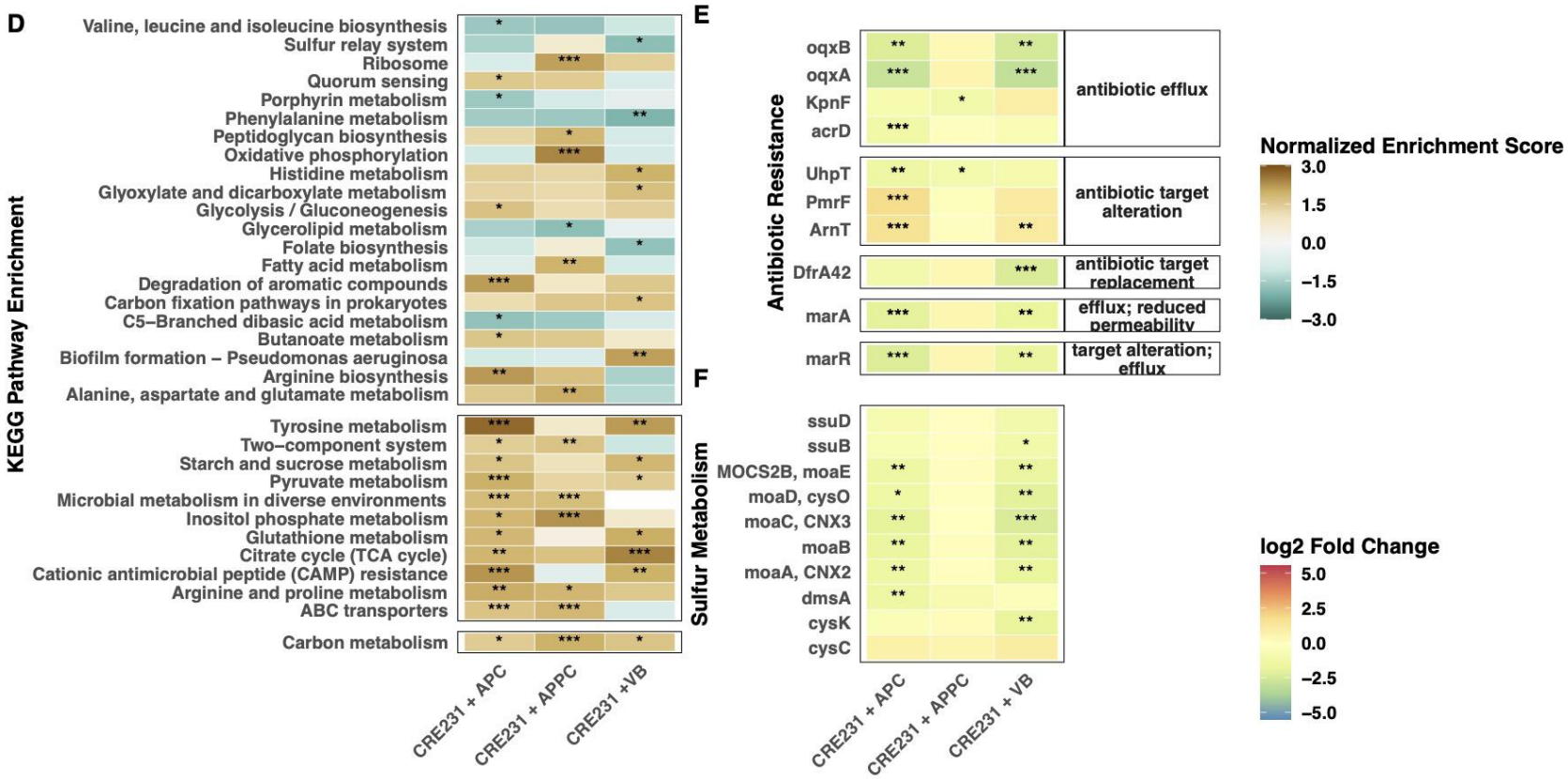
D
KEGG Pathway Enrichment
Valine, leucine and isoleucine biosynthesis
Sulfur relay system
Ribosome
Quorum sensing
Porphyrin metabolism
Phenylalanine metabolism
Peptidoglycan biosynthesis
Oxidative phosphorylation
Histidine metabolism
Glyoxylate and dicarboxylate metabolism
Glycolysis / Gluconeogenesis
Glycerolipid metabolism
Folate biosynthesis
Fatty acid metabolism
Degradation of aromatic compounds
Carbon fixation pathways in prokaryotes
C5–Branched dibasic acid metabolism
Butanoate metabolism
Biofilm formation – Pseudomonas aeruginosa
Arginine biosynthesis
Alanine, aspartate and glutamate metabolism
Tyrosine metabolism
Two–component system
Starch and sucrose metabolism
Pyruvate metabolism
Microbial metabolism in diverse environments
Inositol phosphate metabolism
Glutathione metabolism
Citrate cycle (TCA cycle)
Cationic antimicrobial peptide (CAMP) resistance
Arginine and proline metabolism
ABC transporters
Carbon metabolism
CRE231 + APC
CRE231 + APPC
CRE231 +VB
E
Antibiotic Resistance
oqxB
oqxA
KpnF
acrD
antibiotic efflux
UhpT
PmrF
ArnT
antibiotic target alteration
DfrA42
antibiotic target replacement
marA
efflux; reduced permeability
marR
target alteration; efflux
F
Sulfur Metabolism
ssuD
ssuB
MOCS2B, moaE
moaD, cysO
moaC, CNX3
moaB
moaA, CNX2
dmsA
cysK
cysC
CRE231 + APC
CRE231 + APPC
CRE231 + VB
Normalized Enrichment Score
3.0
1.5
0.0
−1.5
−3.0
log2 Fold Change
5.0
2.5
0.0
−2.5
−5.0

445

446 Figure 4. KEGG pathway enrichment results for samples collected under ambient
447 temperature and humidity condition (A, D), log_2 fold change of genes associated with
448 antibiotic/antimicrobial resistance (B, E), and sulfur metabolism (C, F), compared to no-
449 cleaning samples (ABBL18 or CRE231). KEGG pathways shown here were statistically
450 enriched in at least one of the cleaning conditions (Benjamini-Hochberg corrected p-
451 value ≤ 0.05). Normalized enrichment score (NES) accounts for differences in gene set
452 size and were used to compare enrichment results across KEGG pathways; a positive
453 NES suggests an overall positive up-regulation of genes belonging to its corresponding
454 pathway[32,51,52]. * $p<0.05$, ** $p< 0.01$, and ***$p < 0.001$.
455
456 3.6. *Effects of elevated temperature and humidity on pathogen cell motility and biofilm formation*
457
458 Although over 1,000 differentially expressed genes were identified from *A. baumannii* or *K.*
459 *pneumoniae* transcriptomes between the two temperature and humidity conditions, the majority
460 of the KEGG pathways were composed of genes that were both up-regulated and down-
461 regulated, rendering non-significant results for most pathways. Several exceptions include xylene
462 degradation and oxidative phosphorylation, which were down-regulated in *A. baumannii* samples
463 (Figure 5A, ABBL18 Wet vs ABBL18 Ambient); pentose and glucuronate interconversions,
464 phenylalanine metabolism, quorum sensing, which were up-regulated; and histidine, inositol
465 phosphate, and porphyrin metabolism, which were down-regulated in *K. pneumoniae* samples
466 (Figure 5D, CRE231 Wet vs CRE231 Ambient).
467

468 Under the elevated temperature and humidity condition, the *A. baumannii* transcriptome with
469 APPC was positively enriched with four pathways related to energy production (oxidative
470 phosphorylation), biosynthesis of secondary metabolites (e.g., aerobactin) and metabolism (e.g.,
471 propanoate, glyoxylate, and dicarboxylate). Metabolic pathways, such as toluene, benzoate,
472 chlorocyclohexane, and chlorobenzene, were suppressed (Figure 5A, APPC Wet vs ABBL18
473 Wet). Under elevated temperature and humidity, 16 KEGG pathways related to metabolism (10),
474 membrane transport (3), biosynthesis (2) and translation (1) were enriched in samples with
475 probiotic cleaner (APPC) compared to no-cleaning *K. pneumoniae* samples. Pathways related to
476 valine, leucine and isoleucine biosynthesis and sulfur metabolism were suppressed (Figure 5D,
477 APPC Wet vs CRE231 Wet). This corresponded to the PCA and PERMANOVA results where
478 environmental conditions (temperature and humidity) affected the transcriptome profiles of *K.*
479 *pneumoniae* more than *A. baumannii*.
480
481 In addition to the impact on sulfur metabolism (Figure 5C and Figure 4C) discussed in the
482 previous section, increased moisture availability likely resulted in an increase in *A. baumannii*
483 cell motility through Type IV Pili (Figure 5B) without APPC. Increased moisture availability
484 might also induce a downregulation of osmo-regulation genes such as *envZ* (osmolarity sensor
485 protein, $\log_2$ fold change = -1.38) and *betT2* (osmo-dependent choline transporter $\log_2$ fold
486 change = -2.14). Type 1 pili help mediate colonization by pathogens and promotes host-pathogen
487 interaction as an important virulence factor[53,54]. Some type 1 pilus genes (fimA_1, fim, and smf-
488 1) were expressed in *K. pneumoniae*, but none were found to be differentially expressed under
489 different cleaning scenarios or under elevated temperature and humidity (Figure S6D). Although
490 elevated temperature and humidity did not affect pilus-associated genes, 19 genes related to

491 biofilm formation were differentially expressed in *K. pneumoniae* samples (Figure 5D, CRE231
492 Wet vs CRE231 Ambient), with 14 down-regulated and 5 up-regulated genes. In addition, the
493 quorum sensing pathway, which affects biofilm formation of *K. pneumoniae*[55] , was enriched
494 under elevated temperature and humidity (Figure 5E, CRE231 Wet vs CRE231 Ambient). This
495 indicated that elevated temperature and humidity could assist the persistence of *K. pneumoniae*
496 on surfaces (Figure 2B) by altering the biofilm formation related gene expression. The effects of
497 APPC on *K. pneumoniae* were likely to be masked by the changes due to higher temperature and
498 humidity (Figure 5E), meaning the benefits of probiotic cleaning products could be more limited
499 in tropical areas.
500
501 Our results demonstrated the persistence of probiotic *Bacillus* included in the All-Purpose
502 Probiotic Cleaner up to 72 hours after cleaning, owing to the ability of *Bacillus* spores to survive
503 unfavorable conditions. *A. baumannii* on surfaces cleaned using chemical-based detergent with
504 and without probiotic *Bacillus* contained a comparable amount of viable pathogens, possibly due
505 to the small percentage of germinated *Bacillus* cells and/or slow germination rate on surfaces.
506 The transcriptome of *A. baumannii* with and without probiotic addition shared a high degree of
507 similarity in overall gene expression, including reduced material synthesis and surface activities.
508 On the contrary, the transcriptome of *K. pneumoniae* with probiotic addition showed a high
509 degree of differences compared to samples with chemical cleaner or vegetative *Bacillus*,
510 including reduced response in genes related to antimicrobial resistance, sulfur metabolism and
511 biofilm formation. Longer persistence of viable pathogens on surfaces and reduced effects of
512 APPC on *K. pneumoniae* overall gene expressions with and without cleaners under elevated
513 temperature and humidity suggests that vigilant indoor climate control could contribute to

infection prevention in healthcare-associated scenarios. As the idea of using probiotic microorganisms to promote health benefits becomes increasingly attractive in the field of household cleaning, current understanding on the mechanism and implication of probiotic cleaning remains limited.

Acknowledgement

This work was supported, in whole or in part, by the Bill & Melinda Gates Foundation INV-004298. Under the grant conditions of the Foundation, a Creative Commons Attribution 4.0 Generic License has already been assigned to the Author Accepted Manuscript version that might arise from this submission. JH is supported in part by a Terminal Year Fellowship from the Northwestern University McCormick School of Engineering. The authors would like to thank Marina Zelivyanskaya and Dr. Alan R. Hauser for providing clinical isolates of *Acinetobacter baumannii* and *Klebsiella pneumoniae*. We further thank Andreas Wagner for his assistance.

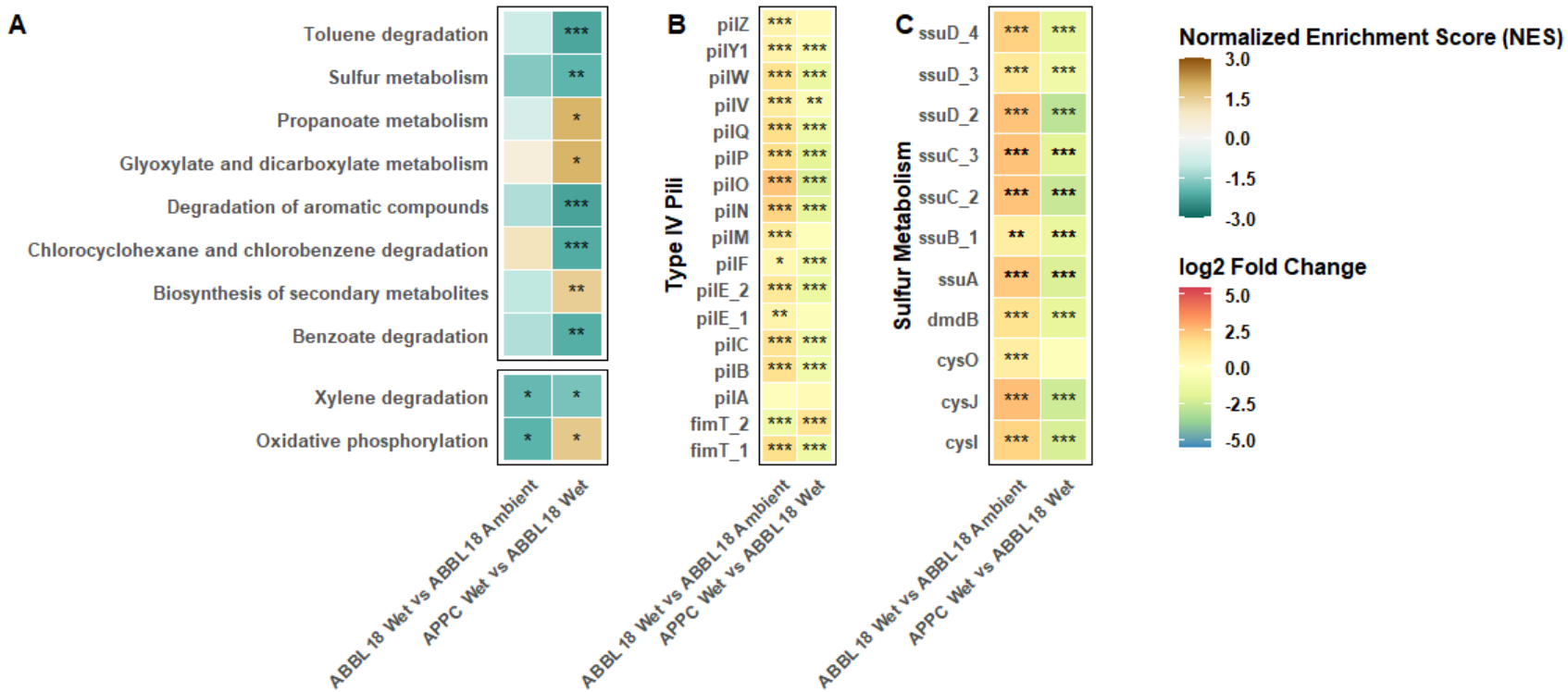
A
Toluene degradation
Sulfur metabolism
Propanoate metabolism
Glyoxylate and dicarboxylate metabolism
Degradation of aromatic compounds
Chlorocyclohexane and chlorobenzene degradation
Biosynthesis of secondary metabolites
Benzoate degradation
Xylene degradation
Oxidative phosphorylation
ABBL 18 Wet vs ABBL 18 Ambient
APPC Wet vs ABBL 18 Wet
B
Type IV Pili
piIZ
piIY1
piIW
piIV
piIQ
piIP
piIO
piIN
piIM
piIF
piIE_2
piIE_1
piIC
piIB
piIA
fimT_2
fimT_1
C
Sulfur Metabolism
ssuD_4
ssuD_3
ssuD_2
ssuC_3
ssuC_2
ssuB_1
ssuA
dmdB
cysO
cysJ
cysI
Normalized Enrichment Score (NES)
3.0
1.5
0.0
-1.5
-3.0
log2 Fold Change
5.0
2.5
0.0
-2.5
-5.0

528

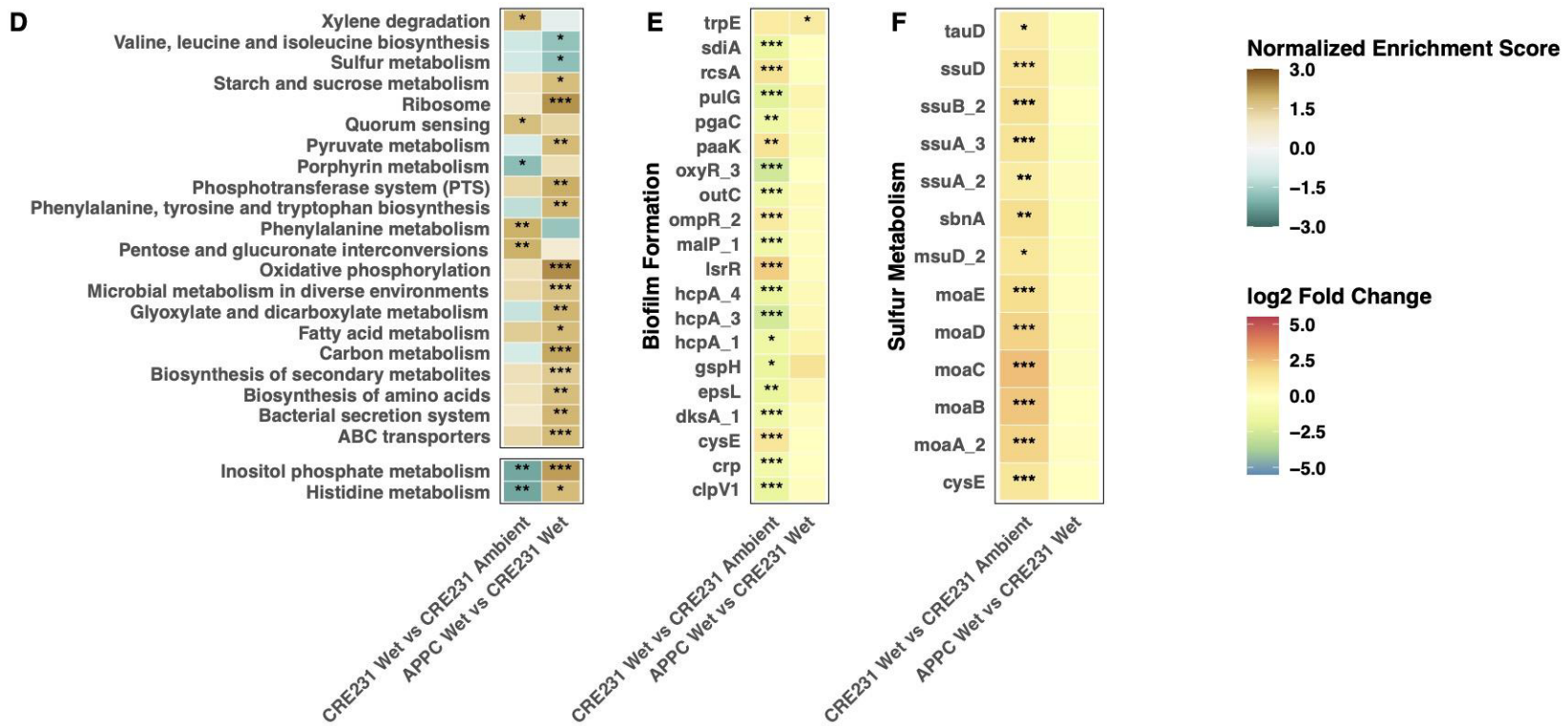

Figure 5. KEGG pathway enrichment results for no-cleaning and APPC samples collected under elevated temperature and humidity condition (A, D), $\log_2$ fold change of genes associated with *Acinitobacter baumannii* cell motility (B), *Klebsiella pneumonia*e biofilm formation (E), and sulfur metabolism (C, F). KEGG pathways shown here were statistically enriched in at least one of the cleaning conditions (Benjamini-Hochberg corrected p-value ≤ 0.05). * $p<0.05$, ** $p< 0.01$, ***$p < 0.001$.

536 References

537

538 1. Navon-Venezia, S., Kondratyeva, K. & Carattoli, A. Klebsiella pneumoniae: a major worldwide
539 source and shuttle for antibiotic resistance. *FEMS Microbiol. Rev.* **013**, 252–275 (2017).

540 2. Hussein, K. *et al.* Impact of carbapenem resistance on the outcome of patients' hospital-acquired
541 bacteraemia caused by Klebsiella pneumoniae. *J. Hosp. Infect.* **83**, 307–313 (2013).

542 3. Kramer, A., Schwebke, I. & Kampf, G. How long do nosocomial pathogens persist on inanimate
543 surfaces? A systematic review. *BMC Infect. Dis.* **6**, 1–8 (2006).

544 4. Velazquez, S. *et al.* From one species to another: A review on the interaction between chemistry
545 and microbiology in relation to cleaning in the built environment. *Indoor Air* **29**, 880–894 (2019).

546 5. Barber, O. W. & Hartmann, E. M. Benzalkonium chloride: A systematic review of its
547 environmental entry through wastewater treatment, potential impact, and mitigation strategies.
548 *Crit. Rev. Environ. Sci. Technol.* **0**, 1–30 (2021).

549 6. Hora, P. I., Pati, S. G., McNamara, P. J. & Arnold, W. A. Increased Use of Quaternary Ammonium
550 Compounds during the SARS-CoV-2 Pandemic and Beyond: Consideration of Environmental
551 Implications. *Environ. Sci. Technol. Lett.* **7**, 622–631 (2020).

552 7. Hayden, M. K. *et al.* Reduction in acquisition of vancomycin-resistant enterococcus after
553 enforcement of routine environmental cleaning measures. *Clin. Infect. Dis. an Off. Publ. Infect.*
554 *Dis. Soc. Am.* **42**, 1552–1560 (2006).

555 8. Sitzlar, B. *et al.* An environmental disinfection odyssey: evaluation of sequential interventions to
556 improve disinfection of Clostridium difficile isolation rooms. *Infect. Control Hosp. Epidemiol.* **34**,

557 459–465 (2013).

558 9. Quinn, M. M. *et al.* Cleaning and disinfecting environmental surfaces in health care: Toward an
559 integrated framework for infection and occupational illness prevention. *Am. J. Infect. Control* **43**,
560 424–434 (2015).

561 10. Al-Marzooq, F. *et al.* Can probiotic cleaning solutions replace chemical disinfectants in dental
562 clinics? *Eur. J. Dent.* **12**, 532–539 (2018).

563 11. Caselli, E. *et al.* Impact of a probiotic-based hospital sanitation on antimicrobial resistance and
564 HAI-associated antimicrobial consumption and costs: a multicenter study. *Infect. Drug Resist.* **12**,
565 501–510 (2019).

566 12. Caselli, E. *et al.* Impact of a Probiotic-Based Cleaning Intervention on the Microbiota Ecosystem
567 of the Hospital Surfaces: Focus on the Resistome Remodulation. *PLoS One* **11**, 1–19 (2016).

568 13. Falagas, M. E. & Makris, G. C. Probiotic bacteria and biosurfactants for nosocomial infection
569 control: a hypothesis. *J. Hosp. Infect.* **71**, 301–306 (2009).

570 14. Suez, J., Zmora, N., Segal, E. & Elinav, E. The pros, cons, and many unknowns of probiotics. *Nat.*
571 *Med.* **25**, 716–729 (2019).

572 15. Andualem, Z., Gizaw, Z., Bogale, L. & Dagne, H. Indoor bacterial load and its correlation to
573 physical indoor air quality parameters in public primary schools. *Multidiscip. Respir. Med.* **14**, 2
574 (2019).

575 16. Elshaghabee, F. M. F., Rokana, N., Gulhane, R. D., Sharma, C. & Panwar, H. Bacillus As Potential
576 Probiotics: Status, Concerns, and Future Perspectives. *Front. Microbiol.* **8**, 1490 (2017).

577 17. Elisashvili, V., Kachlishvili, E. & Chikindas, M. L. Recent Advances in the Physiology of Spore

578 Formation for Bacillus Probiotic Production. *Probiotics Antimicrob. Proteins* **11**, 731–747 (2019).

579 18. Vandini, A. *et al.* Hard Surface Biocontrol in Hospitals Using Microbial-Based Cleaning Products.
580 *PLoS One* **9**, 1–13 (2014).

581 19. Hu, J. *et al.* Impacts of indoor surface finishes on bacterial viability. *Indoor Air* **29**, 551–562
582 (2019).

583 20. Song, W. *et al.* Modified CHROMagar Acinetobacter medium for direct detection of multidrug-
584 resistant Acinetobacter strains in nasal and rectal swab samples. *Ann. Lab. Med.* **33**, 193–195
585 (2013).

586 21. Bankevich, A. *et al.* SPAdes: a new genome assembly algorithm and its applications to single-cell
587 sequencing. *J. Comput. Biol.* **19**, 455–477 (2012).

588 22. Seemann, T. Prokka: rapid prokaryotic genome annotation. *Bioinformatics* **30**, 2068–2069 (2014).

589 23. Jia, B. *et al.* CARD 2017: expansion and model-centric curation of the comprehensive antibiotic
590 resistance database. *Nucleic Acids Res.* **45**, D566–D573 (2017).

591 24. Uritskiy, G. V, DiRuggiero, J. & Taylor, J. MetaWRAP—a flexible pipeline for genome-resolved
592 metagenomic data analysis. *Microbiome* **6**, 158 (2018).

593 25. Parks, D. H., Imelfort, M., Skennerton, C. T., Hugenholtz, P. & Tyson, G. W. CheckM: assessing the
594 quality of microbial genomes recovered from isolates, single cells, and metagenomes. *Genome*
595 *Res.* **25**, 1043–1055 (2015).

596 26. Chaumeil, P.-A., Mussig, A. J., Hugenholtz, P. & Parks, D. H. GTDB-Tk: a toolkit to classify genomes
597 with the Genome Taxonomy Database. *Bioinformatics* **36**, 1925–1927 (2020).

598 27. Kopylova, E., Noé, L. & Touzet, H. SortMeRNA: fast and accurate filtering of ribosomal RNAs in

599 metatranscriptomic data. *Bioinformatics* **28**, 3211–3217 (2012).

600 28. Kim, D., Langmead, B. & Salzberg, S. L. HISAT: a fast spliced aligner with low memory
601 requirements. *Nat. Methods* **12**, 357–360 (2015).

602 29. Liao, Y., Smyth, G. K. & Shi, W. featureCounts: an efficient general purpose program for assigning
603 sequence reads to genomic features. *Bioinformatics* **30**, 923–930 (2014).

604 30. Love, M. I., Huber, W. & Anders, S. Moderated estimation of fold change and dispersion for RNA-
605 seq data with DESeq2. *Genome Biol.* **15**, 550 (2014).

606 31. Kanehisa, M., Sato, Y. & Morishima, K. BlastKOALA and GhostKOALA: KEGG Tools for Functional
607 Characterization of Genome and Metagenome Sequences. *J. Mol. Biol.* **428**, 726–731 (2016).

608 32. Yu, G., Wang, L.-G., Han, Y. & He, Q.-Y. clusterProfiler: an R package for comparing biological
609 themes among gene clusters. *OMICS* **16**, 284–287 (2012).

610 33. Fenollar, F. & Mediannikov, O. Emerging infectious diseases in Africa in the 21st century. *New*
611 *microbes new Infect.* **26**, S10–S18 (2018).

612 34. Stubbendieck, R. M. & Straight, P. D. Multifaceted Interfaces of Bacterial Competition. *J.*
613 *Bacteriol.* **198**, 2145–2155 (2016).

614 35. Butaitė, E., Baumgartner, M., Wyder, S. & Kümmerli, R. Siderophore cheating and cheating
615 resistance shape competition for iron in soil and freshwater Pseudomonas communities. *Nat.*
616 *Commun.* **8**, 414 (2017).

617 36. Hsieh, P.-F., Lu, Y.-R., Lin, T.-L., Lai, L.-Y. & Wang, J.-T. Klebsiella pneumoniae Type VI Secretion
618 System Contributes to Bacterial Competition, Cell Invasion, Type-1 Fimbriae Expression, and In
619 Vivo Colonization. *J. Infect. Dis.* **219**, 637–647 (2019).

620 37. Struve, C., Bojer, M. & Krogfelt, K. A. Characterization of Klebsiella pneumoniae type 1 fimbriae
621 by detection of phase variation during colonization and infection and impact on virulence. *Infect.*
622 *Immun.* **76**, 4055–4065 (2008).

623 38. Itoh, Y. *et al.* Roles of pgaABCD genes in synthesis, modification, and export of the Escherichia
624 coli biofilm adhesin poly-beta-1,6-N-acetyl-D-glucosamine. *J. Bacteriol.* **190**, 3670–3680 (2008).

625 39. Wang, X., Preston, J. F. 3rd & Romeo, T. The pgaABCD locus of Escherichia coli promotes the
626 synthesis of a polysaccharide adhesin required for biofilm formation. *J. Bacteriol.* **186**, 2724–
627 2734 (2004).

628 40. Chuanchuen, R., Narasaki, C. T. & Schweizer, H. P. The MexJK efflux pump of Pseudomonas
629 aeruginosa requires OprM for antibiotic efflux but not for efflux of triclosan. *J. Bacteriol.* **184**,
630 5036–5044 (2002).

631 41. Morita, Y., Cao, L., Gould, V. C., Avison, M. B. & Poole, K. nalD encodes a second repressor of the
632 mexAB-oprM multidrug efflux operon of Pseudomonas aeruginosa. *J. Bacteriol.* **188**, 8649–8654
633 (2006).

634 42. Rosenfeld, N., Bouchier, C., Courvalin, P. & Périchon, B. Expression of the resistance-nodulation-
635 cell division pump AdeIJK in Acinetobacter baumannii is regulated by AdeN, a TetR-type
636 regulator. *Antimicrob. Agents Chemother.* **56**, 2504–2510 (2012).

637 43. C., B. M. M. *et al.* Beyond Antimicrobial Resistance: Evidence for a Distinct Role of the AcrD Efflux
638 Pump in Salmonella Biology. *MBio* **7**, e01916-16 (2021).

639 44. Sharma, A., Sharma, R., Bhattacharyya, T., Bhando, T. & Pathania, R. Fosfomycin resistance in
640 Acinetobacter baumannii is mediated by efflux through a major facilitator superfamily (MFS)
641 transporter-AbaF. *J. Antimicrob. Chemother.* **72**, 68–74 (2017).

642 45. van der Ploeg, J. R. *et al.* Identification of sulfate starvation-regulated genes in Escherichia coli: a
643 gene cluster involved in the utilization of taurine as a sulfur source. *J. Bacteriol.* **178**, 5438–5446
644 (1996).

645 46. Khleifat, K. M. Biodegradation of sodium lauryl ether sulfate (SLES) by two different bacterial
646 consortia. *Curr. Microbiol.* **53**, 444–448 (2006).

647 47. van der Ploeg, J. R., Eichhorn, E. & Leisinger, T. Sulfonate-sulfur metabolism and its regulation in
648 Escherichia coli. *Arch. Microbiol.* **176**, 1–8 (2001).

649 48. Dhouib, A., Hamad, N., Hassaïri, I. & Sayadi, S. Degradation of anionic surfactants by Citrobacter
650 braakii. *Process Biochem.* **38**, 1245–1250 (2003).

651 49. Hu, J. & Hartmann, E. M. Anthropogenic chemicals and their impacts on microbes living in
652 buildings. *Microb. Biotechnol.* **14**, 798–802 (2021).

653 50. Eton & Lepore. 基因的改变NIH Public Access. *Bone* **23**, 1–7 (2008).

654 51. Subramanian, A. *et al.* Gene set enrichment analysis: a knowledge-based approach for
655 interpreting genome-wide expression profiles. *Proc. Natl. Acad. Sci. U. S. A.* **102**, 15545–15550
656 (2005).

657 52. Mootha, V. K. *et al.* PGC-1alpha-responsive genes involved in oxidative phosphorylation are
658 coordinately downregulated in human diabetes. *Nat. Genet.* **34**, 267–273 (2003).

659 53. Rosen, D. A. *et al.* Utilization of an intracellular bacterial community pathway in Klebsiella
660 pneumoniae urinary tract infection and the effects of FimK on type 1 pilus expression. *Infect.*
661 *Immun.* **76**, 3337–3345 (2008).

662 54. Spaulding, C. N. *et al.* Functional role of the type 1 pilus rod structure in mediating host-pathogen

663 interactions. *Elife* **7**, (2018).

664 55. De Araujo, C., Balestrino, D., Roth, L., Charbonnel, N. & Forestier, C. Quorum sensing affects
665 biofilm formation through lipopolysaccharide synthesis in Klebsiella pneumoniae. *Res. Microbiol.*
666 **161**, 595–603 (2010).

667